10.1161/CIRCULATIONAHA.120.046761

Oxidation of Protein Kinase A Regulatory Subunit PKARIα Protects Against Myocardial Ischemia-Reperfusion Injury by Inhibiting Lysosomal-Triggered Calcium Release

Running Title: *Simon et al.; Cardioprotective Effects of Oxidized PKARIα*

Jillian N. Simon, PhD[1]; Besarte Vrellaku MSc[1]; Stefania Monterisi, PhD[2]; Sandy M. Chu, PhD[1]; Nadiia Rawlings, PhD[1]; Oliver Lomas, DPhil, MRCP[1]; Gerard A. Marchal, MSc[1]; Dominic Waithe, PhD[3]; Fahima Syeda, PhD[4]; Parag R. Gajendragadkar, MPhil, MRCP[1]; Raja Jayaram, MD, DPhil[1]; Rana Sayeed, PhD, FRCS[5]; Keith M. Channon, MD, FRCP[1]; Larissa Fabritz, MD[4,6]; Pawel Swietach, DPhil [2]; Manuela Zaccolo, MD, PhD[2]; Philip Eaton, PhD[7]; Barbara Casadei MD, DPhil, FRCP [1]

[1]Division of Cardiovascular Medicine, Radcliffe Department of Medicine, University of Oxford, Oxford, UK; [2]Department of Physiology, Anatomy and Genetics, University of Oxford, Oxford, UK; [3]Wolfson Imaging Centre, Weatherall Institute of Molecular Medicine, University of Oxford, Oxford, UK; [4]Institute of Cardiovascular Sciences, University of Birmingham, Birmingham, UK; [5]Cardiothoracic Surgery, Oxford Heart Centre, Oxford University Hospitals NHS Foundation Trust, Oxford, UK; [6]Department of Cardiology, University Hospitals Birmingham, Birmingham, UK; [7]William Harvey Research Institute, Barts and The London School of Medicine & Dentistry, Queen Mary University of London, Charterhouse Square, London, UK

Address for Correspondence:
Jillian N. Simon, PhD
Division of Cardiovascular Medicine
Radcliffe Department of Medicine
University of Oxford
John Radcliffe Hospital
L6, West Wing
Oxford, UK OX3 9DU
Email: jillian.simon@cardiov.ox.ac.uk

This work was presented as an abstract at the American Heart Association Scientific Sessions, November 13 to November 17, 2020.

Abstract

Background: Kinase oxidation is a critical signalling mechanism through which changes in the intracellular redox state alter cardiac function. In the myocardium, type-1 protein kinase A (PKARIα) can be reversibly oxidized, forming interprotein disulfide bonds within the holoenzyme complex. However, the effect of PKARIα disulfide formation on downstream signaling in the heart, particularly under states of oxidative stress such as ischemia and reperfusion (I/R), remains unexplored.
Methods: Atrial tissue obtained from patients before and after cardiopulmonary bypass and reperfusion and left ventricular (LV) tissue from mice subjected to I/R or sham surgery were used to assess PKARIα disulfide formation by immunoblot. To determine the impact of disulfide formation on PKARIα catalytic activity and sub-cellular localization, live-cell fluorescence imaging and stimulated emission depletion super-resolution microscopy were performed in *prkar1* knock-out mouse embryonic fibroblasts, neonatal myocytes or adult LV myocytes isolated from 'redox dead' (Cys17Ser) PKARIα knock-in mice and their wild-type littermates. Comparison of intracellular calcium dynamics between genotypes was assessed in fura2-loaded LV myocytes whereas I/R-injury was assessed *ex vivo*.
Results: In both humans and mice, myocardial PKARIα disulfide formation was found to be significantly increased (2-fold in humans, $p=0.023$; 2.4-fold in mice, $p<0.001$) in response to I/R *in vivo*. In mouse LV cardiomyocytes, disulfide-containing PKARIα was not found to impact catalytic activity, but instead led to enhanced A-kinase-anchoring protein (AKAP) binding with preferential localization of the holoenzyme to the lysosome. Redox-dependent regulation of lysosomal two pore channels (TPC) by PKARIα was sufficient to prevent global calcium release from the sarcoplasmic reticulum in LV myocytes, without affecting intrinsic ryanodine receptor leak or phosphorylation. Absence of I/R-induced PKARIα disulfide formation in "redox dead" knock-in mouse hearts resulted in larger infarcts (2-fold, $p<0.001$) and a concomitant reduction in LV contractile recovery (1.6-fold, $p<0.001$), which was prevented by administering the lysosomal TPC inhibitor Ned-19 at the time of reperfusion.
Conclusions: Disulfide-modification targets PKARIα to the lysosome where it acts as a gatekeeper for TPC-mediated triggering of global calcium release. In the post-ischemic heart, this regulatory mechanism is critical for protecting from extensive injury and offers a novel target for the design of cardioprotective therapeutics.

Key Words: Redox; calcium signaling; reperfusion injury; protein kinase A phosphorylation; lysosome

Non-standard Abbreviations and Acronyms:

AKAP	A-kinase anchoring protein
FRAP	Fluorescence Recovery After Photobleaching
FRET	Fluorescence Resonance Energy Transfer
I/R	Ischemia/reperfusion
KI	Knock-in
LV	Left ventricle
LVDP	Left ventricular developed pressure
MEFs	Mouse embryonic fibroblasts
NAADP	Nicotinic acid adenine dinucleotide phosphate

NCX	Sodium/calcium exchanger
NRVM	Neonatal rat ventricular myocytes
PKA	Protein kinase A
PKA_{cat}	Protein kinase A, catalytic subunit
PKARIα	Regulatory subunit Iα-containing protein kinase A
PLB	Phospholamban
ROS	Reactive oxygen species
RyR	Ryanodine receptor
SERCA	Sarcoplasmic/endoplasmic reticulum Ca^{2+} ATPase
SR	Sarcoplasmic reticulum
STED	Stimulation emission depletion microscopy
TPC	Two-pore channel
WT	Wild-type

Clinical Perspective

What is new?

- We offer the first evidence that I/R injury, in humans and in mice, induces PKARIα oxidation and disulfide formation.
- Disulfide formation enhances PKARIα intracellular anchoring and promotes compartmentation of the holoenzyme complex to the lysosome, where it acts as a negative regulator of two-pore channel-dependent calcium release.
- Using genetic loss of PKARIα disulfide formation, we demonstrate that this newly identified regulatory mechanism serves as a crucial, adaptive response to myocardial I/R injury by inhibiting excess calcium release and limiting infarct size.

What are the clinical implications?

- Inhibition of lysosomal two-pore channel-dependent calcium release by oxidized PKARIα prevents myocardial cell death in response to I/R, revealing a previously unrecognized mechanism of cardioprotection which could be exploited for therapeutic intervention.

Introduction

Oxidative stress plays a pivotal role in the pathogenesis of ischemia-reperfusion (I/R) injury, with early bursts of reactive oxygen species (ROS) initiating a cascade of deleterious cellular processes which promote cell death and cardiac dysfunction[1, 2]. Paradoxically, inhibition of ROS generation by specific oxidase systems exacerbates I/R injury[3, 4], suggesting that some degree of ROS formation is necessary for cardioprotection[2, 5]. Evidence that ROS underpin the effects of preconditioning or some cardioprotective compounds[6-8] supports this conclusion, as does the general failure of antioxidants to reduced reperfusion injury after coronary angioplasty[9] or improve clinical outcomes in patients with acute myocardial infarction or heart failure[10]. Whilst it is known that ROS signaling is largely mediated through covalent modification of specific cysteine thiols within redox-sensitive proteins[11], the exact mechanisms through which they exert their cardioprotective actions remains unclear.

Protein kinase A (PKA) is one of the master regulatory molecules in the heart. Under physiological conditions, PKA contributes to the cardiac response to catecholamine stimulation through catalyzed phosphorylation of proteins involved in excitation-contraction coupling, metabolism and cardiomyocyte hypertrophy[12, 13]. In disease states, however, persistent activation of PKA signaling, or altered expression of PKA isotypes, has been linked to maladaptive remodelling, pathological hypertrophy and the progression to heart failure[14], making pharmacological targeting of PKA an attractive therapy for the treatment of cardiac disease.

The ability for PKA to regulate a multitude of cellular processes occurs through differential expression and localization of two distinct isotypes (type-1 and type-2) comprised of two catalytic (PKA_{cat}) and two regulatory subunits (RIα or RIβ and RII, respectively)[15]. Although all PKA isotypes depend on cAMP binding for activation, recent work has shown that

type-1 PKA (herein PKARIα) possesses two cysteine residues within the RIα subunits that are sensitive to ROS-mediated oxidation[16, 17]. Studies in isolated hearts and cardiomyocytes, using exogenous oxidants, have shown that oxidation of these cysteines leads to formation of an interprotein disulfide bond within the RIα subunit [17], which may enhance the holoenzyme's catalytic activity, independent of cAMP, or promote PKARIα subcellular targeting[16, 18]. Beyond this, however, little else is known about the endogenous triggers of PKARIα disulfide formation in the myocardium or its functional impact on cardiac function.

Here, we provide the first evidence for endogenous induction of PKARIα disulfide formation in the heart, occurring after I/R in both humans and mice. Using high spatial and temporal resolution imaging modalities, in conjunction with a "redox dead" PKARIα knock-in (KI) mouse model[19], we demonstrate that disulfide modification targets PKARIα to the lysosome, where it acts as a gatekeeper for two-pore channel (TPC)-mediated calcium (Ca^{2+}) release and prevents inappropriate triggering of Ca^{2+} release from the sarcoplasmic reticulum (SR). In the post-ischemic heart, we find that inhibition of lysosomal Ca^{2+} release by oxidized PKARIα is crucial for limiting infarct size and preserving cardiac function during reperfusion, offering a novel target for the design of cardioprotective therapeutics.

Methods

Supporting data and methods can be found in the online-only supplement and will be made available, upon reasonable request, by contacting the corresponding author.

Human samples

Biopsies of the right atrial appendage were obtained before and after cardiopulmonary bypass and reperfusion in patients undergoing on-pump coronary artery bypass surgery at the John

Radcliffe Hospital (Oxford, UK). The study was approved by the Research Ethics Committee (REC reference: 07/Q1607/38) and all patients gave written, informed consent

Animals

"Redox dead" PKARIα KI mice (C57BL/6 background), in which the nucleotides encoding for cysteine at position 17 were mutated to nucleotides encoding for serine (Cys17Ser), were generated as previously described[19]. Only male mice were used for assessment of infarct size. For all other studies, KI mice (12–18 weeks old) of both sexes were compared with their wildtype (WT) littermates. All experiments involving animals were carried out in accordance with the UK Home Office Guidance on the Operation of Animals (Scientific Procedures) Act, 1986 and approved by the Ethics Committee at the University of Oxford.

Statistical analysis

All experimentation and data analysis, apart from immunoblots, were conducted blinded to genotype and intervention. Data were checked for normality of distribution prior to statistical analysis using a Shapiro-Wilk's normality test. Comparisons between data were performed using either a Student's t-test or analysis of variance (ANOVA) with Bonferroni correction (normally distributed) or by the Mann-Whitney test or Kruskal-Wallis test (non-normally distributed). For Ca^{2+} handling data in cardiomyocytes, analyses were carried out in RStudio using a hierarchical statistical method[20], taking in to consideration clustering of single cells per animal and correcting for this in the statistical analysis. The incidence of spontaneous Ca^{2+} release events was compared using Fisher's exact test. A p-value <0.05 was considered statistically significant.

Results

Myocardial I/R promotes PKARIα disulfide formation

Although PKARIα disulfide formation is known to occur in the heart in response to exogenous oxidant treatment[16-18], no evidence for endogenous induction of PKARIα oxidation and disulfide formation has been reported. We therefore sought to determine whether, in humans and mice, disease states associated with increased ROS production would promote PKARIα disulfide bond formation. Atrial tissue biopsies taken from patients undergoing on-pump cardiac surgery showed a minimal degree of PKARIα disulfide formation prior to cardiopulmonary bypass (*pre*); however, in samples acquired from the same patient minutes after cardioplegia and reperfusion (*post-I/R*) the PKARIα disulfide state was found to be significantly increased (**Figure 1A,B**).

Left ventricular (LV) tissue obtained from mice undergoing transient coronary artery ligation *in vivo* also displayed markedly enhanced PKARIα disulfide formation as compared to sham-operated mice, with increased PKARIα oxidation seen in both the I/R and the remote region of the LV (**Figure 1C,D**). Control experiments in human and mouse tissue showed a reduction of high molecular weight bands when samples were treated with reducing agents (*Figure I-A,B in the Supplement*), confirming that the higher molecular weight bands were, indeed, disulfide dimerized PKARIα. In mice, a second band just above the putative RIα monomer was also found following reduction. Further experiments revealed this to be a non-specific band no longer present when PKARIα was purified using cAMP-affinity capture (*Figure IC in the Supplement*). Importantly, unlike oxidative modifications which lead to protein degradation[21], PKARIα oxidation was not associated with loss of total PKARIα protein levels (as observed in *Figure I-A,B in the Supplement*), suggesting that this modification is regulatory in nature and likely has a functional role during I/R-injury.

RIα disulfide formation enhances PKA intracellular anchoring via A-kinase anchoring protein (AKAP) binding without affecting catalytic activity.

For several kinases, regulatory oxidation of cysteine thiols increases their catalytic activity[21]. To test whether this was the case for PKARIα, we used real-time monitoring of PKA catalytic activity by the genetically encoded AKAR3ev Fluorescence Resonance Energy Transfer (FRET) biosensor, which we expressed in cultured adult LV cardiomyocytes isolated from PKARIα "redox dead" KI mice or their WT littermates. Importantly, prior to use of the KI mouse model for mechanistic studies, detailed cardiac characterization was undertaken to ruled out gross structural cardiac remodelling (*Figure II,A-D in the Supplement*), neurohumoral abnormalities (*Figure II,E-H in the Supplement*) or alterations in baseline cardiac function (*Table I in the Supplement*).

As demonstrated in **Figure 2A,** genetic substitution of a serine for one of the critical, disulfide-forming cysteines in the RIα subunit (Cys17Ser)[19] prevented KI mice from forming PKARIα disulfide bonds, either under basal conditions or in response to hydrogen peroxide (H_2O_2) treatment. By contrast, freshly isolated WT cardiomyocytes showed a significant proportion of RIα in the disulfide state under basal conditions (52.6 ± 3.6%), which was further increased by treatment with H_2O_2 (83.0 ± 2.1%). Despite this marked difference in PKARIα disulfide state between WT and KI cardiomyocytes, we found no change in the normalized FRET ratio over the course of the eight minutes H_2O_2 incubation (**Figure 2B,C**). Addition of saturating doses of forskolin and 3-isobutyl-1-methylxanthine (IBMX) at the end of each protocol confirmed that the sensor responded appropriately to a rise in intracellular cAMP and further indicated that no oxidant-induced potentiation of forskolin/IBMX activation occurred. (**Figure 2C**).

Cardiomyocyte culture itself, which was necessary to allow adenoviral gene transduction of the FRET sensor, was associated with a significant increase in the proportion of RIα disulfide formation (up to 72.1 ± 5.8% after 24 h in culture; **Figure 2D**). In fact, PKARIα was found to be highly oxidized following culture or storage of cells under all *ex vivo* conditions assessed (*Table II in the Supplement*). As the near-complete induction of disulfide bond formation by culturing could have accounted for the failure of PKARIα activity to increase in response to H_2O_2, we also tested whether, in WT cardiomyocytes, PKARIα exhibited greater intrinsic catalytic compared to KI, as evaluated using the H89-inhibitable fraction. As shown in **Figure 2E**, the FRET response to H89 did not differ between WT and KI cardiomyocytes, consistent with the overall conclusion that disulfide formation has no direct impact on PKARIα catalytic activity.

Given that disulfide bonds form within the AKAP binding domain of the RIα subunit[22], we asked whether PKARIα intracellular anchoring was impacted by the oxidation state. To assess this we conducted Fluorescence Recovery After Photobleaching (FRAP) experiments – which offer the robust capability of measuring protein diffusion and mobility in live cells[23] – in PKARIα knock-out mouse embryonic fibroblasts (*prkar1a*$^{-/-}$ MEFs) expressing GFP-tagged WT or mutant RIα proteins. The use of *prkar1a*$^{-/-}$ MEFs allowed us to monitor changes in intracellular anchoring of GFP-tagged PKARIα in the absence of endogenous PKARIα, which might compete for available AKAP binding sites. Non-reduced immunoblotting confirmed the presence of disulfide bond formation in cells expressing PKARIα(WT) or in those cells expressing PKARIα(H24A), a mutation known to substantially reduce PKARIα AKAP-binding affinity without impacting disulfide formation[22], but not in PKARIα(C17S)-expressing cells (*Figure III-A in the Supplement*).

Compared to PKARIα(WT), PKARIα(C17S) showed a higher degree of GFP-PKARIα diffusive exchange within the photobleached region-of-interest (ROI), as indicated by the higher Recovery Index (**Figure 3A**). This difference was reflected quantitatively as a reduction in the immobile (i.e. anchored) fraction of PKARIα in C17S-expressing cells compared to WT (**Figure 3B,C**), indicating that, in the absence of disulfide formation, less PKARIα is restricted to intracellular compartments. Indeed, the relative reduction in the immobile fraction for PKARIα(C17S)-expressing cells was equivalent to that found in PKARIα(H24A)-expressing cells (**Figure 3C**). Diffusion rate constants for the mobile fraction of PKARIα were also calculated from the FRAP curves, but found not to differ between mutant and WT PKARIα (*Figure III-B in the Supplement*).

To test whether the reduction in immobile PKARIα(C17S) was due to a loss of disulfide-dependent anchoring to endogenous AKAPs, we repeated the FRAP experiments in cells expressing each of the constructs (WT or C17S) in combination with the RIα anchoring disruptor (RIAD) which prevents PKARIα interaction with AKAPs, with 50-fold selectivity over PKARII[24]. In cells expressing PKARIα(WT), disruption of AKAP-binding by RIAD led to a reduction in the immobile fraction of PKARIα to levels comparable to PKARIα(C17S)-expressing cells (**Figure 3D,E**). The effect of RIAD was only present in PKARIα(WT)-expressing cells, with no significant effect of RIAD on cells expressing the "redox dead" RIα (C17S) mutant (**Figure 3E**). As before, we saw no effect of the C17S mutant or RIAD on the diffusion rates of the mobile fraction of RIα (*Figure III-C in the Supplement*). Thus, the disulfide state of RIα appears to influence the extent to which PKA is anchored within the cell, via AKAP binding, without affecting the diffusion rate of PKARIα's cytosolic fraction or its catalytic activity.

PKARIα disulfide formation localizes the holoenzyme to lysosomal microdomains in cardiomyocytes

If PKARIα disulfide formation affects AKAP-mediated intracellular anchoring, then the disulfide state would also be expected to influence PKARIα subcellular compartmentation; however, to-date the identity of these compartments has remained elusive. Taking advantage of the oxidizing conditions of cell culture, which was shown to induce near-complete PKARIα disulfide formation, we determined whether the disulfide state influenced PKARIα subcellular compartmentation in cardiomyocytes using immunofluorescence imaging in cultured WT and KI LV cardiomyocytes. In WT cardiomyocytes, PKARIα was found to co-localize with mitochondria, the nucleus (*Figure IV-A in the Supplement*) and LAMP-2 positive lysosomes (**Figure 4A,B**). Whereas confocal microscopy was sufficient to demonstrate that localization to the mitochondria and nucleus was unaffected by the loss of PKARIα disulfide formation in KI cardiomyocytes (*Figure IVB in the Supplement*), super-resolution Stimulation Emission Depletion (STED) microscopy was required to quantify the extent of PKARIα association with the lysosome, and assess the redox-dependence of this interaction.

STED imaging allowed accurate identification of lysosomes (**Figure 4C-E**) – whose average diameter is less than the 200 nm resolution of standard confocal imaging – and significantly improved quantification of PKARIα fluorescence intensity at nanometer distances[25]. By quantifying PKARIα fluorescence intensity at increasing radial distances from lysosomal foci (**Figure 4F**; radial increments=70 nm as determined in *Figure V-A in the Supplement*) and comparing that to the PKARIα fluorescence intensity measured at randomly generated coordinates, we were able to demonstrate significant clustering of PKARIα to within 70nm of lysosomes in WT cardiomyocytes (**Figure 4G**, *Figure V-B in the Supplement*). Using

the same approach, we found that PKA_{cat} also clustered near lysosomes (**Figure 4H,I**), indicating that the entire holoenzyme complex was present in the lysosomal microdomain when PKA was highly oxidized. By contrast, in the absence of disulfide formation (ie., KI cardiomyocytes), PKARIα no longer clustered near lysosomes (**Figure 5A**). Clustering of PKA_{cat} was also found to be reduced in KI cardiomyocytes, albeit to a lesser extent (**Figure 5B**; p-value for significant interaction=0.009). The loss of PKA clustering to the lysosome, however, did not appear to impact gross lysosomal distribution (*Figure V-C in the Supplement*).

We next assessed whether clustering of PKARIα to the lysosomal was mediated by AKAP binding. For this, STED imaging experiments were repeated using the RIAD disruptor peptide in neonatal rat cardiomyocytes (NRVMs), which are more easily cultured and transfected than adult mouse cardiomyocytes. As with adult LV cardiomyocytes, control-transfected NRVMs showed a high degree of PKARIα clustering to LAMP2-positive lysosomes (**Figure 5C,D**). RIAD transfection significantly reduced this colocalization – particularly at the nearest measureable distance – whereas transfection of cells with SuperAKAP-IS, a potent and specific disruptor of PKA-RII:AKAP interactions, did not (**Figure 5C,E**).

Collectively, these data provide strong evidence that induction of PKARIα disulfide formation facilitates localization of the holoenzyme complex to the lysosome of cardiomyocytes in a manner which is AKAP-dependent.

Intracellular Ca^{2+} release is regulated by PKARIα through its interaction with the lysosomal TPCs

Lysosomes are known to couple with the mitochondria[26] and the cardiomyocyte SR[27], forming structural microdomains through which lysosomal Ca^{2+} release may impact Ca^{2+} handling by these organelles[26, 28]. We initially assessed, therefore, whether loss of lysosomal-localized

PKARIα in KI cardiomyocytes affected mitochondrial or SR Ca^{2+} handling (e.g. release and reuptake) under steady-state conditions. As before, we found that the conditions required to assess intracellular Ca^{2+} handling in WT cardiomyocytes led to near-complete induction of PKARIα disulfide formation (94.5 ± 2.3%; as reported in *Table II in the Supplement*). Direct measurement of mitochondrial Ca^{2+} handling (at 37°C) in permeabilized cardiomyocytes loaded with Rhod-2 showed equivalent levels of mitochondrial Ca^{2+} loading in WT and KI cells challenged with 100 nmol/L free [Ca^{2+}] (*Figure VI-A,B in the Supplement*). Likewise, similar rates of mitochondrial Ca^{2+} efflux were observed between genotypes (*Figure VI-C in the Supplement*) indicating that mitochondrial Ca^{2+} handling was unaffected by PKARIα displacement from the lysosome.

Under steady-state pacing (3 Hz; 35±1°C), fura-2 loaded cardiomyocytes showed no significant differences in the intracellular Ca^{2+} ($[Ca^{2+}]_i$) transient amplitude or diastolic $[Ca^{2+}]_i$ levels between genotypes, although a mild increase in the rate of intracellular Ca^{2+} decay was observed in KI cardiomyocytes (**Figure 6A-D**). Derivation of the Ca^{2+} ATPase (SERCA) and Na^+/Ca^{2+} exchanger (NCX)-dependent rate constants for free intracellular Ca^{2+} decay indicated a mild enhancement of SERCA-dependent uptake of Ca^{2+} into the SR in KI cardiomyocytes (**Figure 6E**), independent of phospholamban (PLB) phosphorylation or an altered PLB:SERCA ratio (*Figure VII A-D in the Supplement*). However, measurement of total SR Ca^{2+} content, using rapid caffeine application, showed no genotype-dependent differences (**Figure 6F**), indicating that the modest increase in SERCA-mediated Ca^{2+} reuptake had no significant impact on SR Ca^{2+} loading under these conditions. In agreement with these findings, echocardiographic parameters of LV function were similar in both genotypes (as reported in *Table I in the Supplement*). Equally, we saw no genotype differences in fractional shortening or the rate of

relaxation of isolated cardiomyocytes (*Figure VII E-G in the Supplement*), in the peak and kinetics of the L-type Ca^{2+} current ($I_{Ca,L}$) (**Figure 6G,H**) or in the NCX current (**Figure 6I**). Nevertheless, KI cardiomyocytes displayed a higher incidence of spontaneous Ca^{2+} release events during a pause from steady-state pacing (**Figure 6J-L**), suggesting that the displacement of PKARIα from the lysosomal microdomain in KI cardiomyocytes may be leading to dysregulated lysosomal Ca^{2+} release sufficient to directly trigger RyR opening. For this to occur, close physical proximity between the two structures would have to take place. Indeed, STED imaging confirmed that LAMP-2 positive lysosomes were closely coupled with RyRs (**Figure 7A,B**), with nearest-neighbor distance histograms in WT and KI cardiomyocytes showing the majority of the lysosomes lying in close (i.e. <200nm) proximity to RyRs, with no significant difference between genotypes (**Figure 7B**).

We therefore assessed the dynamics of intracellular Ca^{2+} release from RyR by perfusing WT or KI cardiomyocytes with a $0Na^{+}/0Ca^{2+}$ extracellular solution (which prevents triggering of RyR opening from extracellular sources) and included the use of the reversible RyR inhibitor, tetracaine, to allow for simultaneous quantification of intrinsic RyR Ca^{2+} leak. Cardiomyocytes showed stable Ca^{2+} transient recordings under tetracaine perfusion, with no spontaneous events occurring in either genotype under these conditions. However, following tetracaine washout a significantly high proportion of KI cardiomyocytes developed dramatic Ca^{2+} oscillations (**Figure 7C,D**). No differences in the RyR leak/load relationship (an indirect assessment of RyR opening probability[29]; **Figure 7E**) or PKA-mediated RyR phosphorylation (*Figure VII-H in the Supplement*) was found between genotypes, indicating that the Ca^{2+} oscillations were unlikely to be driven by inherent changes in RyR opening. By contrast, depletion of lysosomal Ca^{2+} stores using acute bafilomycin A1 treatment completely abolished Ca^{2+} oscillations under $0Na^{+}/0Ca^{2+}$

conditions (**Figure 7F**), while competitive inhibition of Ca^{2+}-permeable lysosomal TPCs using Ned-19 significantly attenuated the incidence of Ca^{2+} oscillations (**Figure 7G**). Importantly, measurement of SR Ca^{2+} load (in non-oscillating cells) indicated that the ability of either drug to prevent global SR Ca^{2+} oscillations was not a consequence of reduced SR Ca^{2+} content (*Figure VII I-J in the Supplement*), supporting the conclusion that these events were a direct result of spontaneous lysosomal Ca^{2+} release from TPCs, occurring when PKARIα was no longer localized to the lysosome.

Despite the presence of spontaneous SR Ca^{2+} release in KI cardiomyocytes, we did not observe an increase in pacing-induced ventricular arrhythmias in these mice (*Figure VIII-A in the Supplement*). Likewise, there was no evidence for induction of Ca^{2+}-activated stress responses in KI hearts. Specifically, transcript levels for multiple markers of the unfolded protein response – a conserved system of ER-stress signaling cascades activated in response to protein misfolding or altered SR/ER Ca^{2+} content – showed no evidence of increased transcriptional activation in KI LVs (*Figure VIII-B in the Supplement*). KI LVs also showed no marked difference in the conversion of LC3-I to LC3-II or degradation of p62 (*Figure VIII-C in the Supplement*) which, together, indicated activation of the autophagosome-lysosome pathway was not altered in these mice.

Redox-dependent regulation of lysosomal Ca^{2+} release by PKARIα is cardioprotective against I/R injury

SR Ca^{2+} oscillations are known to occur in the initial period of myocardial reperfusion, leading to cell death and LV dysfunction[30]. Given our observation that PKARIα disulfide formation is induced shortly after myocardial reperfusion in humans and mice, we posited that inhibition of global Ca^{2+} release by oxidized, lysosomally-targeted PKARIα may confer cardioprotection in

the post-ischemic heart. To test this hypothesis, hearts from WT and KI mice were subjected to *ex vivo* I/R, with LV function measured throughout and infarct size assessed following the 60 min reperfusion (**Figure 8A**). Further, to determine the contribution of TPC-dependent lysosomal Ca^{2+} release, hearts of either genotype were administered Ned-19 (or DMSO vehicle) at the time of reperfusion.

Although no difference in LV hemodynamic measurements were seen during the baseline stabilization period (*Table III in the Supplement*), KI hearts administered vehicle at reperfusion showed significantly lower LV developed pressures (LVDP) throughout the reperfusion period (**Figure 8B**) and displayed 2-fold larger infarcts compared to WTs (**Figure 8C,D**). Absence of differences in PKA-dependent RyR phosphorylation during I/R (*Figure IX in the Supplement*) ruled out the possibility that direct alterations in RyR accounted for the poorer outcome in vehicle-treated KI mice. Instead, inhibition of lysosomal Ca^{2+} release, by addition of Ned-19 at the time of reperfusion, was sufficient to restore both contractile function and infarct size in KI hearts to levels comparable to WT, with no further protective effects observed in WT hearts. These findings are consistent, therefore, with a model in which disulfide-modified PKARIα limits I/R-induced Ca^{2+} overload by decreasing lysosomal triggering of global SR Ca^{2+} release.

Discussion

Our findings lead us to three major conclusions: 1) PKARIα disulfide formation is a consistent and conserved response to myocardial I/R injury *in vivo*, occurring both in humans and mice; 2) oxidation of PKARIα serves as a means to compartmentalize PKARIα within the lysosomal microdomain where it acts as an inhibitor of TPC-dependent Ca^{2+} release; 3) this regulatory

mechanism is an adaptive response to I/R which allows the heart to limit the extent of injury and aid functional recovery.

Functional impact of PKARIα disulfide formation on kinase function and localization

Although redox-modification of several kinases has been shown to promote catalytic activation[21], our data rule out the possibility that PKARIα disulfide formation has the same effect. Instead, we provide strong evidence that the principal regulatory function of PKARIα disulfide formation is to promote localization of the holoenzyme complex to distinct subcellular compartments via enhanced AKAP binding. This conclusion is at odds with some previous studies, which report increased PKA activity in response to elevations in ROS[31, 32] and reactive nitrogen species[33]. However, the observed changes in PKA catalytic activity were inferred from downstream functional readouts – some of which have important limitations[34] – or increased substrate phosphorylation, which make it difficult to distinguish between genuine increases in PKA catalytic activity vs focused subcellular targeting of the enzyme. The use of a genetically-encoded FRET biosensor here, in conjunction with PKARIα KI cardiomyocytes, provided a robust means to directly assess changes in intrinsic catalytic activity with varying degrees of PKARIα disulfide formation, and showed no correlation between the two, suggesting that previous findings may, instead, be a consequence of substrate-induced activation within specific microdomains[35], a characteristic unique to RIα-containing PKA.

The observation that physically restricted pools of PKARIα are lost when disulfide formation is prevented (C17S mutation) argues strongly for a concomitant loss of AKAP-mediated anchoring of PKARIα that is dependent, at least in part, on the structural stability afforded by the disulfide bond[22]. In support of this hypothesis, disruption of RIα-AKAP interaction in FRAP experiments caused significant liberation of PKARIα from the immobile

pool, an effect which was not observed in C17S-expressing cells. Likewise, within the cardiomyocyte C17S mutation, or disruption of AKAP binding using RIAD resulted in displacement of the PKARIα holoenzyme from lysosomes. For the latter, lysosomal localization of PKARIα was shown to be diminished, but not abolished, by RIAD disruption, a finding that may reflect suboptimal concentrations of transfected RIAD in the cells owing to some degree of peptide degradation as reported previously [24].

Regulation of lysosomal Ca^{2+} release by PKARIα

Oxidation-dependent localization of PKARIα to the lysosome represents a significant, and entirely novel, mechanism through which PKA regulates Ca^{2+} release in the heart. Our classic understanding of Ca^{2+} regulation by PKA involves the rapid phosphorylation of key Ca^{2+} handling proteins, including RyR, PLB and the L-type Ca^{2+} channel, which act concordantly to enhance contraction and relaxation. However, several studies suggest that these substrates are uniquely targeted by RII-containing pools of PKA, while activation of PKARIα has little effect on excitation-contraction coupling[36-38]. Consistent with this, we find no evidence for differential phosphorylation of 'classic' PKA targets (e.g. in RyR or PLB), nor do we see differences in cardiomyocyte contractility or LV systolic function *in vivo* or in isolated hearts between WT and KI mice. Instead, we find that the striking Ca^{2+} oscillations and spontaneous Ca^{2+} release events observed in KI cardiomyocytes are due to dysregulated Ca^{2+} release from lysosomal TPCs when PKARIα is absent from this microdomain.

Lysosomal Ca^{2+} efflux can promote SR Ca^{2+} release either by triggering RyRs Ca^{2+} release directly[39] or by enhancing SR Ca^{2+} loading[28]. We observed minimal enhancement of SERCA-mediated Ca^{2+} uptake in KI cardiomyocytes, with no obvious difference in SR Ca^{2+} load or RyR leak compared to WT. Instead, we found spontaneous triggering of SR Ca^{2+} release (in

the absence of sarcolemmal Na^+/Ca^{2+} flux), which could be prevented by inhibiting RyR opening or lysosomal Ca^{2+} release via TPC channels. These findings, and the fact that we found lysosomes lying in close physical proximity to the RyR, indicates that PKARIα directly modulates the crosstalk between lysosomal TPCs and RyRs. Of note, the prevention of SR Ca^{2+} release by these drugs was not driven by a reduction in SR Ca^{2+} load. In fact, in KI cardiomyocytes Ned-19 significantly increased load. As this would be expected to promote Ca^{2+} oscillations by increasing RyR opening probability, it is not likely that the increased load had a direct impact on Ned-19's inhibitory effects.

PKARIα disulfide formation as an adaptive response to I/R

Although early bursts of ROS are thought to be the primary mediators of reperfusion-induced injury[1, 2], evidence indicates that some degree of ROS are needed at the time of reperfusion to protect the heart[4, 5]. In particular, I/R-induced elevations in NOX-derived ROS activate redox signalling pathways that promote cell survival[3, 40, 41]. In this regard, compartmentation of oxidant sources and their downstream targets are suggested to be a discriminating factor between adaptive vs maladaptive signaling[3]. Consistent with this, we observed that disulfide-dependent compartmentation of PKARIα was a necessary event to confer cardioprotection. When this response was lost in KI mice, cardiomyocytes exhibited dysregulated lysosomal Ca^{2+} release, which ultimately led to exacerbated I/R injury.

The fact that pharmacological inhibition of TPCs at the time of reperfusion reduced infarct size and improved functional recovery in KI hearts highlights a causal role for lysosomal Ca^{2+} release in mediating PKARIα's adaptive response to I/R. Inhibition of TPCs, either pharmacologically or by genetic knockdown, has been shown to protect the heart against I/R injury, both *in vitro* and *in vivo* [42]. Interestingly, pharmacological inhibition of TPC conferred

cardioprotection in WT mice only when a more potent derivative of Ned-19, called Ned-K, was used[42]. This may explain why, in keeping with the same report[42], we did not see an added benefit in WT hearts perfused with Ned-19.

Whilst our observations provide strong evidence for a cardioprotective role of oxidized PKARIα, independent of increases in cAMP, it is conceivable that further activation of RIα-containing pools of PKA by cAMP may provide additional protection from I/R injury. Indeed, glucagon-like peptide-1 (GLP-1) and prostaglandin E1 (PGE1), which are currently being tested in clinical trials for their use in treating myocardial infarction[43, 44] and reperfusion-injury[45, 46], have both been found to promote selective activation of RI-, but not RII-containing PKA in cardiomyocytes [36, 38]. Preclinical studies have already shown that the beneficial effects of these hormones rely on PKA[47, 48], although the downstream mechanisms have yet to be fully elucidated. Our findings indicate that inhibition of lysosomal Ca^{2+} release by PKARIα may contribute to the cardioprotective effects of these hormones and further suggest that targeted enhancement of lysosomal PKARIα, or inhibition of TPCs, offer a novel adaptive signalling pathway to exploit for the prevention of I/R injury.

Potential Limitations

Although we showed that disulfide formation is important for restricting PKARIα to lysosomal regions, it is not clear for our data whether regulation of lysosomal function occurs through a direct interaction between PKARIα and TPCs or via more distal PKA-dependent signaling events within this microdomain. *In vitro* PKA can directly phosphorylate TPCs and alter channel opening[49]; whether this occurs *in vivo* and is influenced by PKARIα disulfide formation remains to be explored. Similarly, we cannot exclude that differences in Nicotinic Acid Adenine Dinucleotide Phosphate (NAADP, the ligand for TPC channels) between genotypes may have

contributed to our results. However, this seems unlikely as altered NAADP levels have been shown primarily to increase SR Ca^{2+} loading and Ca^{2+} transient dynamics in cardiomyocytes[50], neither of which were found to be materially different between KI and WT mice. It should also be noted that the contribution of enhanced SR Ca^{2+} oscillations to the exacerbated I/R injury seen in KI mice was inferred from studies in isolated cardiomyocytes, as opposed to a direct assessment during I/R. Nevertheless, our data in KI mice showing that Ned-19 prevents SR Ca^{2+} oscillations in cardiomyocytes and limits myocardial I/R injury strongly supports a link between the two.

Conclusions

Our work identifies, for the first time, oxidation-dependent compartmentation of the PKARIα holoenzyme to the lysosomal microdomain, where it acts as a potent inhibitor of intracellular Ca^{2+} release. In the setting of I/R, where PKARIα disulfide formation is induced, this regulatory mechanism is critical for limiting infarct size and offers a novel target for the design of cardioprotective therapeutics.

Acknowledgments

The authors thank Pablo Hernandez-Varas and Christoffer Langerholm (Wolfson Imaging Centre, University of Oxford) for their expertise in STED microscopy; Ricardo Carnicer, Craig Lygate and Debra McAndrews (University of Oxford) for the provision of LV tissue from mice undergoing *in vivo* I/R or sham surgery; and S. Nashitha Kabir (University of Birmingham) for her technical assistance.

Sources of Funding

This work was supported by the British Heart Foundation (CH/12/3/29609 BC & JNS; RG/11/15/29375 BC & RJ; RG/16/12/32451 BC & BV; FS/17/17/32438 PG; RG/17/6/32944 MZ & SM; PG/15/5/31110, MZ; RG/15/9/31534 PS; RG/12/5/29576, KMC & SC; PG/17/44/33064, PE; Accelerator Award AA/18/2/34218, LF); the NIHR Oxford Biomedical Research Centre (BC); the Medical Research Council (MR/P023150/1 PE; MR/S005382/1, MRC/BBSRC/EPSRC, MR/K01577X/1, DW); the Garfield-Weston Foundation (MPS/IVIMS-11/12-4032, BC & NR); and the Wellcome Trust (0998981Z/12/Z, OL).

Disclosures

None directly related to this work.

Supplemental Materials

Supplemental (Expanded) Methods

Supplemental Table I-III

Supplemental Figure I–IX

References 51-56

References

1. Zweier JL and Talukder MA. The role of oxidants and free radicals in reperfusion injury. *Cardiovasc Res*. 2006;70:181-190.
2. Cadenas S. ROS and redox signaling in myocardial ischemia-reperfusion injury and cardioprotection. *Free Radic Biol Med*. 2018;117:76-89.
3. Matsushima S, Kuroda J, Ago T, Zhai P, Ikeda Y, Oka S, Fong GH, Tian R and Sadoshima J. Broad suppression of NADPH oxidase activity exacerbates ischemia/reperfusion injury through inadvertent downregulation of hypoxia-inducible factor-1alpha and upregulation of peroxisome proliferator-activated receptor-alpha. *Circ Res*. 2013;112:1135-1149.

4. Matsushima S, Tsutsui H and Sadoshima J. Physiological and pathological functions of NADPH oxidases during myocardial ischemia-reperfusion. *Trends Cardiovasc Med*. 2014;24:202-205.
5. Kleikers PW, Wingler K, Hermans JJ, Diebold I, Altenhofer S, Radermacher KA, Janssen B, Gorlach A and Schmidt HH. NADPH oxidases as a source of oxidative stress and molecular target in ischemia/reperfusion injury. *J Mol Med (Berl)*. 2012;90:1391-1406.
6. Chen W, Gabel S, Steenbergen C and Murphy E. A redox-based mechanism for cardioprotection induced by ischemic preconditioning in perfused rat heart. *Circ Res*. 1995;77:424-429.
7. Tritto I, D'Andrea D, Eramo N, Scognamiglio A, De Simone C, Violante A, Esposito A, Chiariello M and Ambrosio G. Oxygen radicals can induce preconditioning in rabbit hearts. *Circ Res*. 1997;80:743-748.
8. Forbes RA, Steenbergen C and Murphy E. Diazoxide-induced cardioprotection requires signaling through a redox-sensitive mechanism. *Circ Res*. 2001;88:802-809.
9. Flaherty JT, Pitt B, Gruber JW, Heuser RR, Rothbaum DA, Burwell LR, George BS, Kereiakes DJ, Deitchman D, Gustafson N, et al. Recombinant human superoxide dismutase (h-SOD) fails to improve recovery of ventricular function in patients undergoing coronary angioplasty for acute myocardial infarction. *Circulation*. 1994;89:1982-1991.
10. Frohlich GM, Meier P, White SK, Yellon DM and Hausenloy DJ. Myocardial reperfusion injury: looking beyond primary PCI. *Eur Heart J*. 2013;34:1714-1722.
11. Paulsen CE and Carroll KS. Cysteine-mediated redox signaling: chemistry, biology, and tools for discovery. *Chem Rev*. 2013;113:4633-4679.
12. Bers DM. Calcium cycling and signaling in cardiac myocytes. *Annu Rev Physiol*. 2008;70:23-49.
13. Muller FU, Boknik P, Knapp J, Linck B, Luss H, Neumann J and Schmitz W. Activation and inactivation of cAMP-response element-mediated gene transcription in cardiac myocytes. *Cardiovasc Res*. 2001;52:95-102.
14. Saad NS, Elnakish MT, Ahmed AAE and Janssen PML. Protein Kinase A as a Promising Target for Heart Failure Drug Development. *Arch Med Res*. 2018;49:530-537.
15. Skalhegg BS and Tasken K. Specificity in the cAMP/PKA signaling pathway. Differential expression,regulation, and subcellular localization of subunits of PKA. *Front Biosci*. 2000;5:D678-693.
16. Brennan JP, Bardswell SC, Burgoyne JR, Fuller W, Schroder E, Wait R, Begum S, Kentish JC and Eaton P. Oxidant-induced activation of type I protein kinase A is mediated by RI subunit interprotein disulfide bond formation. *J Biol Chem*. 2006;281:21827-21836.
17. Brennan JP, Wait R, Begum S, Bell JR, Dunn MJ and Eaton P. Detection and mapping of widespread intermolecular protein disulfide formation during cardiac oxidative stress using proteomics with diagonal electrophoresis. *J Biol Chem*. 2004;279:41352-41360.
18. Burgoyne JR and Eaton P. Transnitrosylating nitric oxide species directly activate type I protein kinase A, providing a novel adenylate cyclase-independent cross-talk to beta-adrenergic-like signaling. *J Biol Chem*. 2009;284:29260-29268.
19. Burgoyne JR, Rudyk O, Cho HJ, Prysyazhna O, Hathaway N, Weeks A, Evans R, Ng T, Schroder K, Brandes RP, et al. Deficient angiogenesis in redox-dead Cys17Ser PKARIalpha knock-in mice. *Nature communications*. 2015;6:7920.
20. Sikkel MB, Francis DP, Howard J, Gordon F, Rowlands C, Peters NS, Lyon AR, Harding SE and MacLeod KT. Hierarchical statistical techniques are necessary to draw reliable

conclusions from analysis of isolated cardiomyocyte studies. *Cardiovasc Res*. 2017;113:1743-1752.
21. Burgoyne JR, Oka S, Ale-Agha N and Eaton P. Hydrogen peroxide sensing and signaling by protein kinases in the cardiovascular system. *Antioxid Redox Signal*. 2013;18:1042-1052.
22. Sarma GN, Kinderman FS, Kim C, von Daake S, Chen L, Wang BC and Taylor SS. Structure of D-AKAP2:PKA RI complex: insights into AKAP specificity and selectivity. *Structure*. 2010;18:155-166.
23. Lippincott-Schwartz J, Snapp EL and Phair RD. The Development and Enhancement of FRAP as a Key Tool for Investigating Protein Dynamics. *Biophys J*. 2018;115:1146-1155.
24. Carlson CR, Lygren B, Berge T, Hoshi N, Wong W, Tasken K and Scott JD. Delineation of type I protein kinase A-selective signaling events using an RI anchoring disruptor. *J Biol Chem*. 2006;281:21535-21545.
25. Hell SW and Wichmann J. Breaking the diffraction resolution limit by stimulated emission: stimulated-emission-depletion fluorescence microscopy. *Opt Lett*. 1994;19:780-782.
26. Peng W, Wong YC and Krainc D. Mitochondria-lysosome contacts regulate mitochondrial Ca(2+) dynamics via lysosomal TRPML1. *Proc Natl Acad Sci U S A*. 2020;117:19266-19275.
27. Aston D, Capel RA, Ford KL, Christian HC, Mirams GR, Rog-Zielinska EA, Kohl P, Galione A, Burton RA and Terrar DA. High resolution structural evidence suggests the Sarcoplasmic Reticulum forms microdomains with Acidic Stores (lysosomes) in the heart. *Sci Rep*. 2017;7:40620.
28. Capel RA, Bolton EL, Lin WK, Aston D, Wang Y, Liu W, Wang X, Burton RA, Bloor-Young D, Shade KT, et al. Two-pore Channels (TPC2s) and Nicotinic Acid Adenine Dinucleotide Phosphate (NAADP) at Lysosomal-Sarcoplasmic Reticular Junctions Contribute to Acute and Chronic beta-Adrenoceptor Signaling in the Heart. *J Biol Chem*. 2015;290:30087-30098.
29. Curran J, Hinton MJ, Rios E, Bers DM and Shannon TR. Beta-adrenergic enhancement of sarcoplasmic reticulum calcium leak in cardiac myocytes is mediated by calcium/calmodulin-dependent protein kinase. *Circ Res*. 2007;100:391-398.
30. Garcia-Dorado D, Ruiz-Meana M, Inserte J, Rodriguez-Sinovas A and Piper HM. Calcium-mediated cell death during myocardial reperfusion. *Cardiovasc Res*. 2012;94:168-180.
31. Wagner S, Dantz C, Flebbe H, Azizian A, Sag CM, Engels S, Mollencamp J, Dybkova N, Islam T, Shah AM, et al. NADPH oxidase 2 mediates angiotensin II-dependent cellular arrhythmias via PKA and CaMKII. *J Mol Cell Cardiol*. 2014;75:206-215.
32. Srinivasan S, Spear J, Chandran K, Joseph J, Kalyanaraman B and Avadhani NG. Oxidative stress induced mitochondrial protein kinase A mediates cytochrome c oxidase dysfunction. *PLoS One*. 2013;8:e77129.
33. Beck KF, Euler J, Eisel F, Beck M, Kohler Y, Sha LK, von Knethen A, Longen S and Pfeilschifter J. Cytokines induce protein kinase A-mediated signalling by a redox-dependent mechanism in rat renal mesangial cells. *Biochem Pharmacol*. 2015;93:362-369.
34. Koschinski A and Zaccolo M. Activation of PKA in cell requires higher concentration of cAMP than in vitro: implications for compartmentalization of cAMP signalling. *Sci Rep*. 2017;7:14090.
35. Viste K, Kopperud RK, Christensen AE and Doskeland SO. Substrate enhances the sensitivity of type I protein kinase a to cAMP. *J Biol Chem*. 2005;280:13279-13284.

36. Vila Petroff MG, Egan JM, Wang X and Sollott SJ. Glucagon-like peptide-1 increases cAMP but fails to augment contraction in adult rat cardiac myocytes. *Circ Res*. 2001;89:445-452.
37. Keely SL. Prostaglandin E1 activation of heart cAMP-dependent protein kinase: apparent dissociation of protein kinase activation from increases in phosphorylase activity and contractile force. *Mol Pharmacol*. 1979;15:235-245.
38. Di Benedetto G, Zoccarato A, Lissandron V, Terrin A, Li X, Houslay MD, Baillie GS and Zaccolo M. Protein kinase A type I and type II define distinct intracellular signaling compartments. *Circ Res*. 2008;103:836-844.
39. Boittin FX, Galione A and Evans AM. Nicotinic acid adenine dinucleotide phosphate mediates Ca2+ signals and contraction in arterial smooth muscle via a two-pool mechanism. *Circ Res*. 2002;91:1168-1175.
40. Bell RM, Cave AC, Johar S, Hearse DJ, Shah AM and Shattock MJ. Pivotal role of NOX-2-containing NADPH oxidase in early ischemic preconditioning. *FASEB J*. 2005;19:2037-2039.
41. Jiang S, Streeter J, Schickling BM, Zimmerman K, Weiss RM and Miller FJ, Jr. Nox1 NADPH oxidase is necessary for late but not early myocardial ischaemic preconditioning. *Cardiovasc Res*. 2014;102:79-87.
42. Davidson SM, Foote K, Kunuthur S, Gosain R, Tan N, Tyser R, Zhao YJ, Graeff R, Ganesan A, Duchen MR, et al. Inhibition of NAADP signalling on reperfusion protects the heart by preventing lethal calcium oscillations via two-pore channel 1 and opening of the mitochondrial permeability transition pore. *Cardiovasc Res*. 2015;108:357-366.
43. Bethel MA, Patel RA, Merrill P, Lokhnygina Y, Buse JB, Mentz RJ, Pagidipati NJ, Chan JC, Gustavson SM, Iqbal N, et al. Cardiovascular outcomes with glucagon-like peptide-1 receptor agonists in patients with type 2 diabetes: a meta-analysis. *Lancet Diabetes Endocrinol*. 2018;6:105-113.
44. Nikolaidis LA, Mankad S, Sokos GG, Miske G, Shah A, Elahi D and Shannon RP. Effects of glucagon-like peptide-1 in patients with acute myocardial infarction and left ventricular dysfunction after successful reperfusion. *Circulation*. 2004;109:962-965.
45. Zhu H, Xu X, Ding Y, Zhou L and Huang J. Effects of prostaglandin E1 on reperfusion injury patients: A meta-analysis of randomized controlled trials. *Medicine (Baltimore)*. 2017;96:e6591.
46. Lonborg J, Vejlstrup N, Kelbaek H, Botker HE, Kim WY, Mathiasen AB, Jorgensen E, Helqvist S, Saunamaki K, Clemmensen P, et al. Exenatide reduces reperfusion injury in patients with ST-segment elevation myocardial infarction. *Eur Heart J*. 2012;33:1491-1499.
47. Bose AK, Mocanu MM, Carr RD, Brand CL and Yellon DM. Glucagon-like peptide 1 can directly protect the heart against ischemia/reperfusion injury. *Diabetes*. 2005;54:146-151.
48. Ye Y, Keyes KT, Zhang C, Perez-Polo JR, Lin Y and Birnbaum Y. The myocardial infarct size-limiting effect of sitagliptin is PKA-dependent, whereas the protective effect of pioglitazone is partially dependent on PKA. *Am J Physiol Heart Circ Physiol*. 2010;298:H1454-1465.
49. Lee CS, Tong BC, Cheng CW, Hung HC and Cheung KH. Characterization of Two-Pore Channel 2 by Nuclear Membrane Electrophysiology. *Sci Rep*. 2016;6:20282.
50. Macgregor A, Yamasaki M, Rakovic S, Sanders L, Parkesh R, Churchill GC, Galione A and Terrar DA. NAADP controls cross-talk between distinct Ca2+ stores in the heart. *J Biol Chem*. 2007;282:15302-15311.

51. Whittington HJ, Ostrowski PJ, McAndrew DJ, Cao F, Shaw A, Eykyn TR, Lake HA, Tyler J, Schneider JE, Neubauer S, et al. Over-expression of mitochondrial creatine kinase in the murine heart improves functional recovery and protects against injury following ischaemia-reperfusion. *Cardiovasc Res*. 2018;114:858-869.
52. Carnicer R, Hale AB, Suffredini S, Liu X, Reilly S, Zhang MH, Surdo NC, Bendall JK, Crabtree MJ, Lim GB, et al. Cardiomyocyte GTP cyclohydrolase 1 and tetrahydrobiopterin increase NOS1 activity and accelerate myocardial relaxation. *Circ Res*. 2012;111:718-727.
53. Gold MG, Lygren B, Dokurno P, Hoshi N, McConnachie G, Tasken K, Carlson CR, Scott JD and Barford D. Molecular basis of AKAP specificity for PKA regulatory subunits. *Mol Cell*. 2006;24:383-395.
54. Nadella KS and Kirschner LS. Disruption of protein kinase a regulation causes immortalization and dysregulation of D-type cyclins. *Cancer Res*. 2005;65:10307-10315.
55. Bolte S and Cordelieres FP. A guided tour into subcellular colocalization analysis in light microscopy. *J Microsc*. 2006;224:213-232.
56. Puglisi JL, Bassani RA, Bassani JW, Amin JN and Bers DM. Temperature and relative contributions of Ca transport systems in cardiac myocyte relaxation. *Am J Physiol*. 1996;270:H1772-1778.

Figure Legends

Figure 1. Myocardial I/R induces PKARIα oxidation in humans and mice. (**A**) Immunoblot detection of PKARIα monomers and disulfide dimers, observed under non-reducing conditions, in atrial biopsies taken just prior to cardiopulmonary bypass (*pre*) and again immediately after reperfusion (*post-I/R*) in patients undergoing on-pump cardiac surgery. (**B**) Quantification of the percentage of PKARIα that exists as a disulfide dimer (calculated by the density of PKARIα dimer/(the density of dimer + monomer) and expressed as a percentage of total PKARIα) shows significant elevations in the disulfide state following I/R in humans. Mean ± SD; paired Student's t-test. n=18. (**C**) Immunoblot detection of PKARIα monomers, disulfide dimers and high molecular weight complexes (HMWC), observed under non-reducing condition, in mouse LV samples obtained remotely or downstream of a transient coronary artery ligation (for 45 min occlusion and 30 min reperfusion; 'I/R') or after sham surgery. The presence of a second band above the monomer was found to be a non-specific reaction (*see Online Figure IC*). (**D**) Quantification of the percentage of PKARIα disulfide dimers (calculated as in panel B) shows higher levels of oxidation in the 'I/R' and remote tissue as compared to sham operated hearts. Data are means ± SD; one-way ANOVA; n = 5 for sham, n=4 for Remote and I/R.

Figure 2. PKARIα disulfide bond formation does not impact global catalytic activity. (**A**) Immunoblot detection of PKARIα monomers and disulfide dimers, observed under non-reducing conditions, in WT and KI LV cardiomyocytes treated with vehicle or H_2O_2 (250 μmol/L, 10 min). H_2O_2 induced formation of PKARIα disulfides in WT, but not in KI, cardiomyocytes (isolated from n=11 mice for WT and n=6 for KI). (**B**) Dynamic measurement of PKA activity in

cultured adult mouse cardiomyocytes using the cytosolic FRET AKAR3ev biosensor (expressed as a normalized YFP/CFP FRET ratio, R/R_0) following addition of H_2O_2 (250 µmol/L), during H_2O_2 wash off, and in response to maximal stimulation of cAMP production by forskolin (FRSK; 25µmol/L) plus isobutylmethylxanthine (IBMX; 100µmol/L). Mean ± SEM; two-way ANOVA with repeated measures; $p<0.01$ for time-effect, p-value not significant for genotype or interaction. n = 6-7 cardiomyocytes per group from 4 mice per genotype. (**C**) Quantification of the maximal FRET ratio in WT and KI cardiomyocytes during H_2O_2 and FRSK + IBMX treatment. (**D**) Induction of PKARIα disulfide dimer formation, assessed under non-reducing conditions, following 4h and 24h of culturing. Cardiomyocytes from the same isolation were used for statistical comparison at each time. All data points shown with means ± SEM indicated; one-way ANOVA with Bonferroni's correction; n = 5. (**E**) Assessment of basal PKA activity using the AKAR3ev FRET biosensor and the PKA inhibitor H89 (30 µmol/L) in cardiomyocytes cultured for 24h. Data are means ± SEM; two-way ANOVA with repeated measures; $p<0.01$ for time-effect, p-value not significant for genotype or interaction. n = 6-7 cardiomyocytes per group from 4 mice per genotype.

Figure 3. PKARIα disulfide bond formation enhances intracellular anchoring. (**A**) Expression of the photobleached recovery index, which provides a ratio of GFP- PKARIα fluorescence before bleaching and at the end of the recovery period (per pixel) in *prkar1a*$^{-/-}$ MEF cells expressing WT or C17S PKARIα. FRAP region-of-interest (ROI) as indicated. (**B**) Fluorescence recovery dynamics, with time of bleach and the fraction of fluorescence that does not recovery (e.g. immobile fraction) indicated (**C**) Quantification of the immobile fraction within the ROI (shown with Mean ± SD) for *prkar1a*$^{-/-}$ MEF cells expressing WT (black), C17S

(green) and H24A (pink) GFP-tagged PKARIα. One-way ANOVA; n=30-39 cells per group, from 3 independent passages. (**D**) Fluorescence recovery dynamics and (**E**) quantification of the immobile fraction (shown as Mean ± SD) from *prkar1a*$^{-/-}$ MEF cells expressing WT (black/grey) or C17S (green/light green) in the absence or presence of co-transfection with the RIAD disruptor peptide. Two-way ANOVA with Bonferroni post-test; n = 30-39 cells per group, from 3 independent passages.

Figure 4. Both the RIα and PKA$_{cat}$ subunits are found clustered to the lysosome. (**A**) Representative confocal image (scale bar=5 μm) of a cultured WT mouse LV cardiomyocyte immunostained for PKARIα (yellow) and LAMP2 (magenta), showing diffuse staining of endogenous PKARIα as well as punctate regions of staining (*arrows*). (**B**) Magnified confocal images (scale bar=500 nm) indicate that PKARIα clustering occurs near LAMP-2 positive lysosomes; however (**C**) few lysosomes are identified and their size estimates (full-width half maximum; FWHM) are overestimated by the resolution of standard confocal microscopy. (**D**) Imaging with STED dramatically improves the resolution of LAMP-2 positive lysosomes, with (**E**) increased identification and more reliable size estimates (FWHM). (**F**) To quantify the degree of PKARIα clustering near lysosomes, as captured in STED mode, LAMP-2 positive lysosomes were identified using a custom-build macro in ImageJ (*left*) and the PKARIα intensity quantified at increasing radial distances (green circles) from each lysosome (*right*). For comparisons against cytosolically diffuse PKARIα, the same analysis was repeated on each image using random, computer-generated coordinates. Scale bar=500 nm (**G**) Quantification of PKARIα fluorescence intensity in WT adult mouse cardiomyocytes as a function of distance from the lysosome. Data are means ± SEM; repeated measures two-way ANOVA with

Bonferroni's correction, $p<0.01$ for significant interaction between PKARIα fluorescence intensity and distance from the lysosome; n = 38 cardiomyocytes, each from 3 mice. (**H**) The degree of clustering between PKA_{cat} (green) and LAMP-2 positive lysosomes (magenta) was also assessed by STED imaging in WT cardiomyocytes using the same method as in Panel F. Scale bars=5 μm for whole cell confocal and 1 μm for magnified STED images (**I**) Quantification of PKA_{cat} fluorescence intensity as a function of distance from the lysosome. Data are means ± SEM; repeated measures two-way ANOVA with Bonferroni's correction, $p<0.01$ for significant interaction between PKA_{cat} fluorescence intensity and distance from the lysosome; n = 35 cardiomyocytes, each from 3 mice.

Figure 5. PKARIα shows AKAP-mediated lysosomal clustering when in the disulfide state. (**A**) *Top*, STED imaging of PKARIα (yellow) and LAMP2 (magenta) immunostaining in cardiomyocytes isolated from WT or KI mice. *Bottom*, quantitative comparison of PKARIα intensity in WT and KI cardiomyocytes, normalized for each cell to the cytosolically diffuse intensity, plotted as a function of the radial distance from the lysosome. Normalized data for WT cells was calculated from those included in **Figure 4G**, data shown as means ± SEM; repeated measures two-way ANOVA with Bonferroni's correction, *$p<0.001$ for significant interaction between genotypes and distance; n = 38-41 cardiomyocytes, each from 3 mice/genotype. (**B**) *Top*, STED imaging of PKA_{cat} (green) and LAMP2 (magenta) immunostaining in cardiomyocytes isolated from WT or KI mice. *Bottom*, quantitative comparison of normalized PKA_{cat} intensity in WT and KI cardiomyocytes as a function of the radial distance from the lysosome. Normalized data for WT cells was calculated from those included in **Figure 4I**, data shown as means ± SEM; repeated measures two-way ANOVA with Bonferroni's correction,

*p=0.005 for significant interaction between genotypes and distance; n = 35-37 cardiomyocytes, each from 3 mice/genotype. (**C**) Neonatal rat ventricular myocytes (NRVM) were transfected for 24 h with GFP only (transfection control), GFP + the RI anchoring disruptor, RIAD or GFP + the RII anchoring disruptor, Super-AKAP-IS, and then fixed and co-immunostained for PKARIα (Atto-647, yellow) and LAMP2 (AF-594, magenta). STED images were only acquired in GFP-positive cells. (**D**) PKARIα fluorescent intensity was quantified within a given distance from each lysosome as in **Figure 4F** (binned by Atto-647 resolution; 80 nm). *p<0.0001 for significant interaction, *p<0.001 for difference between foci at 80, 160 and 240 nm distance. (**E**) Comparison of normalized intensities within 80 nm of LAMP-2 positive vesicles was made between cells transfected with GFP only and those transfected with GFP + RIAD or GFP + Super-AKAP-IS. Normalized data for the 'GFP' group were calculated from cells used in **Figure 5D**, data shown as means ± SEM; repeated measures two-way ANOVA with Bonferroni's correction, *p<0.001 for GFP vs GFP + RIAD and #p<0.01 for GFP + RIAD vs GFP + Super-AKAP-IS; n = 28-38 cardiomyocytes, each from 3 independent isolations/condition. For A-C, Scale bar = 1 μm and 500 nm for all magnified images.

Figure 6. KI cardiomyocytes display spontaneous Ca^{2+} release in the absence of changes in SR Ca^{2+} load. (**A**) Electrically stimulated $[Ca^{2+}]_i$ transients (3 Hz, 35±1°C) showed that, compared with WT, KI cardiomyocytes have similar (**B**) $[Ca^{2+}]_i$ transient amplitude and (**C**) diastolic Ca^{2+}, but have (**D**) a significantly faster $[Ca^{2+}]_i$ decay rate (tau). (**E**) Calculated rate constants for $[Ca^{2+}]_i$ decline attributed to SERCA *(left*) and NCX (*right*) show that faster rate of $[Ca^{2+}]_i$ decay in KI cardiomyocytes is driven by faster SERCA-mediated Ca^{2+} uptake, in the

absence of measurable difference in total SR Ca^{2+} load (**F**). All data points are shown, with median and interquartile range (IQR) indicated; statistical analysis was done using a hierarchical model on normally-distributed data. Where data were non-normally distributed, logarithmic transformation was applied prior to statistical testing; n = 8 animals per group, 72 cardiomyocytes per group. Patch-clamping of isolated LV cardiomyocytes showed no difference in (**G**) the peak L-type calcium current ($I_{Ca,L}$), (**H**) $I_{Ca,L}$ activation (*closed circles*) or inactivation (*open circles*) kinetics or (**I**) the NCX peak current (taken at -40mV). n=50 cardiomyocytes, each from 6 mice/genotype. Mann-Whitney test (panel I); repeated measures two-way ANOVA (panel G and H). (**J**) Pace-pause protocol used to assess spontaneous Ca^{2+} release events in WT and KI cardiomyocytes. Example of spontaneous Ca^{2+} release events (SCaREs) shown by arrows. (**K**) Percentage of cardiomyocytes that developed spontaneous Ca^{2+} release events during a 60 second pause from pacing and (**L**) the frequency of events within the 60 secs. Fisher's exact test for panel K and Mann-Whitney test for panel L; n = 110-112 cardiomyocytes, each from 6 mice/genotype.

Figure 7. KI cardiomyocytes display global SR Ca^{2+} oscillations triggered by TPC-mediated lysosomal Ca^{2+} release. (**A**) Whole cell confocal image of a representative adult mouse LV cardiomyocyte co-immunostained for RyR2 (cyan) and LAMP2 (magenta). Imaging in high-resolution STED mode shows close proximity between LAMP2-positive lysosomes and RyR. Scale bars = 1 μm (left zoomed image) and 500 nm (right zoomed image) (**B**) RyR-LAMP2 nearest-neighbor distance distributions in WT and KI cardiomyocytes calculated by measuring the distances from the center of the LAMP2-positive lysosome (or a random, computer generated coordinate as is the case for the 'Rdm-Lyso' histogram) to the center of the nearest RyR cluster.

n= 18-19 cardiomyocytes, each from 3 mice/genotype. Statistical comparison of experimental (WT or KI) vs Rdm-Lyso distributions using a Mann-Whitney's non-parametric test, *p<0.0001. (**C**) Protocol used to assess $[Ca^{2+}]_i$ dynamics and RyR leak simultaneously for panels C-G, with trace showing the development of Ca^{2+} oscillations in a KI cardiomyocyte under 0Na/0Ca conditions. (**D**) The percentage of WT and KI cardiomyocytes per isolation that developed Ca^{2+} oscillations in the presence or absence of tetracaine (10 mmol/L). The Kruskal-Wallis test was used to assess differences between groups; n=13 (WT) and 15 (KI) mice per group. Individual data and their median value are shown. (**E**) Oscillations occurred in the absence of differences in RyR leak, quantified by the RyR leak/SR Ca^{2+} load relationship in WT and KI mouse LV cardiomyocytes. All data points shown with median and IQR; Mann-Whitney non-parametric test; n=24 cardiomoycytes, each from 6-7 mice/genotype. The occurrence rate of Ca^{2+} oscillations was also assessed in cardiomyocytes treated with vehicle (DMSO) vs (**F**) bafilomycin A1 (Bafilo; 100 nmol/L), or (**G**) Ned-19 (5 μmol/L). Fisher's exact test; n=7 mice per group (Bafilo), n=9 mice per group (Ned-19).

Figure 8. Disulfide-modified PKARIα protects the myocardium from I/R injury via its regulation of lysosomal Ca^{2+} release. (**A**) Following baseline stabilization, WT and KI hearts were subjected to 25 mins global ischemia and 60 mins of reperfusion. Either 10 μmol/L Ned-19 or an equivalent volume of DMSO (vehicle) was included in the reperfusion solution. (**B**) Compared to WT hearts, KI hearts showed worse LVDP recovery following I/R, which was prevented by Ned-19 treatment. Data are means ± SEM with statistical comparisons made using two-way ANOVA with Bonferroni's correction for pairwise comparison, *p<0.01 for KI vs WT, #p<0.01 for KI vs KI + Ned-19; n=7-9 hearts per group. (**C** and **D**) Post-I/R infarct size, assessed

by TTC staining and quantified as the percentage of area-at-risk (% AAR), was larger in KI hearts compared to WT; this difference was abolished by adding Ned-19 in the reperfusion solution. For panel C, scale bar = 1cm. All data points are shown with mean ± SD indicated; one-way ANOVA with Bonferroni's correction; n = 5 hearts per group.

Figure 1

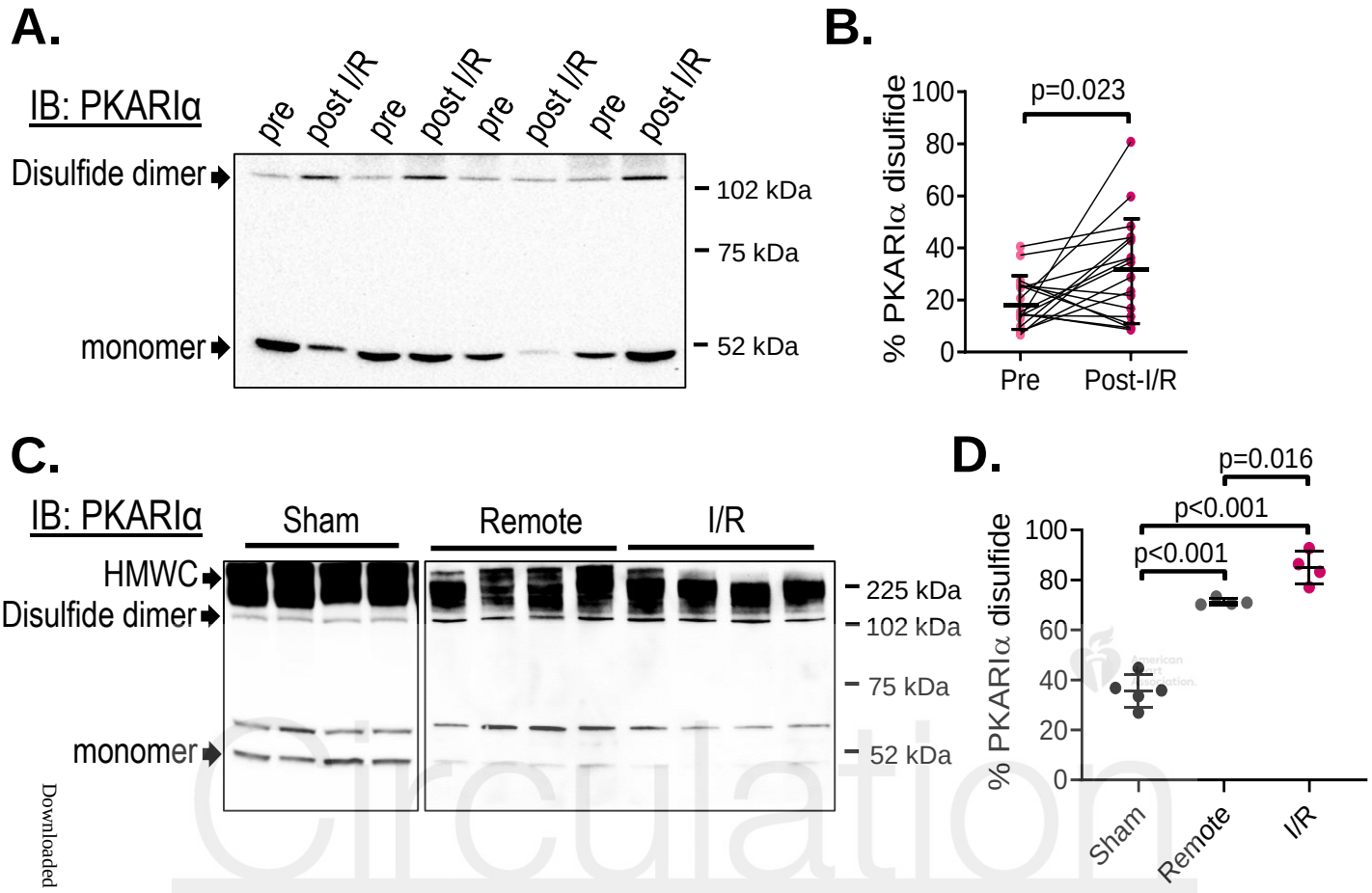

Figure 2

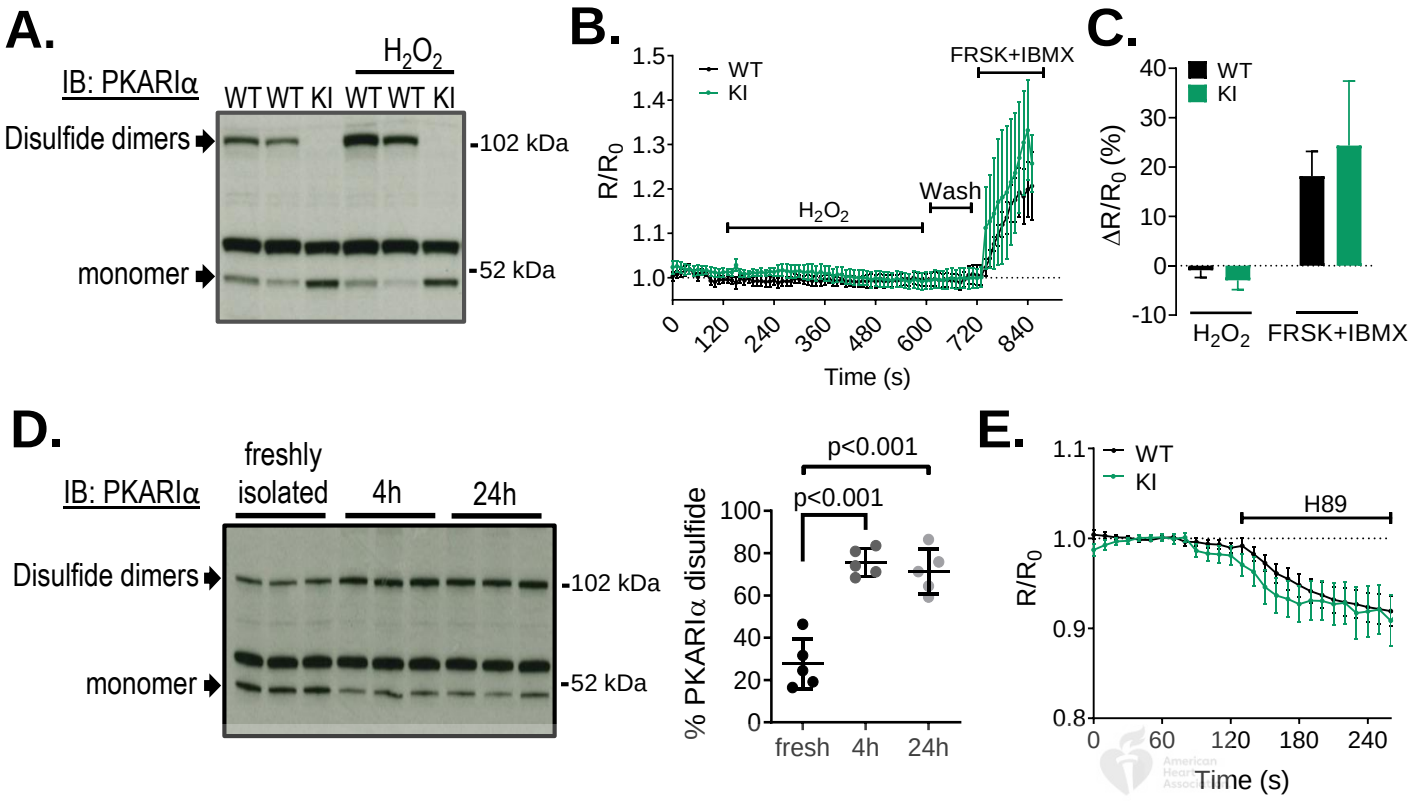

Figure 3

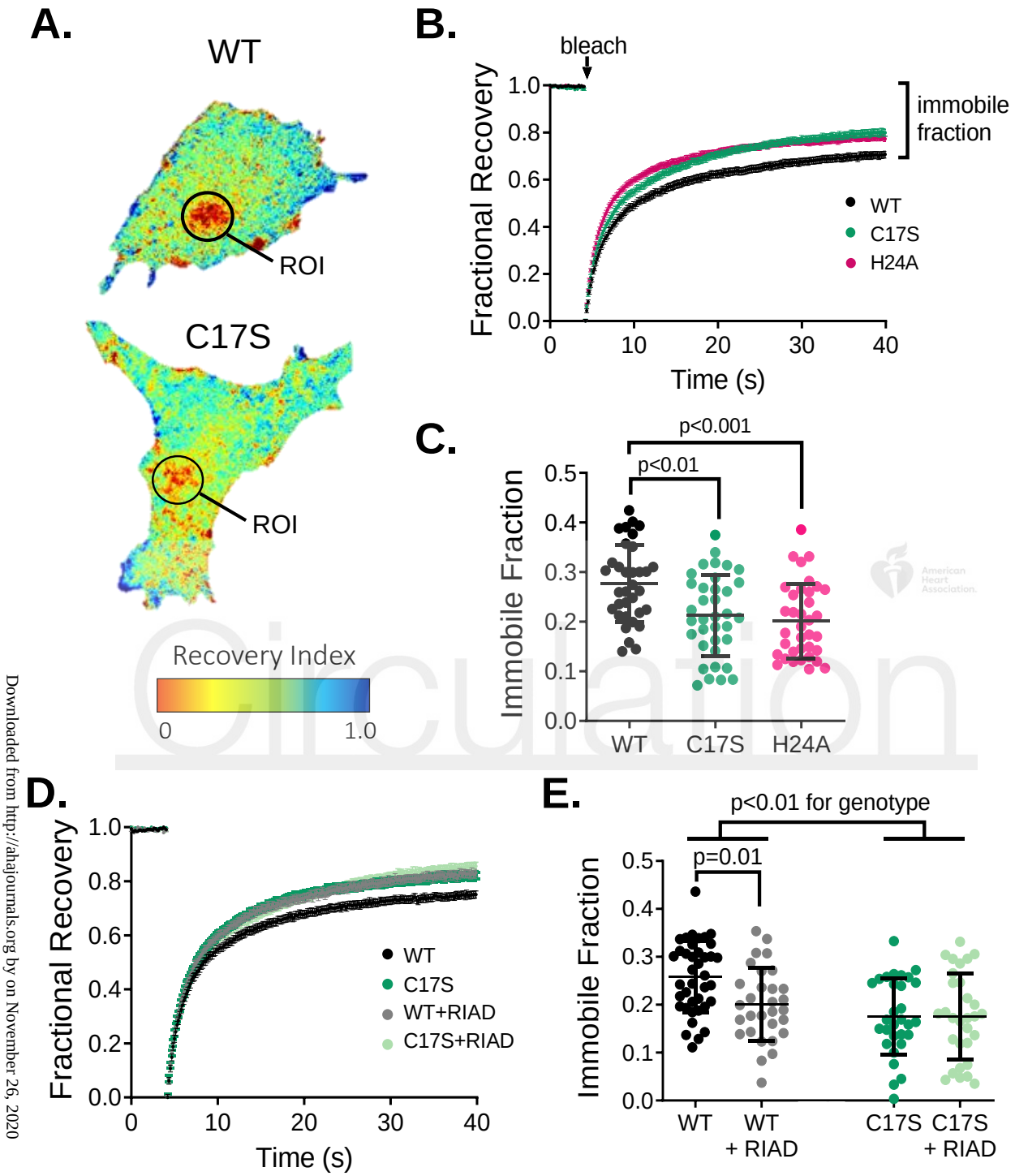

Figure 4

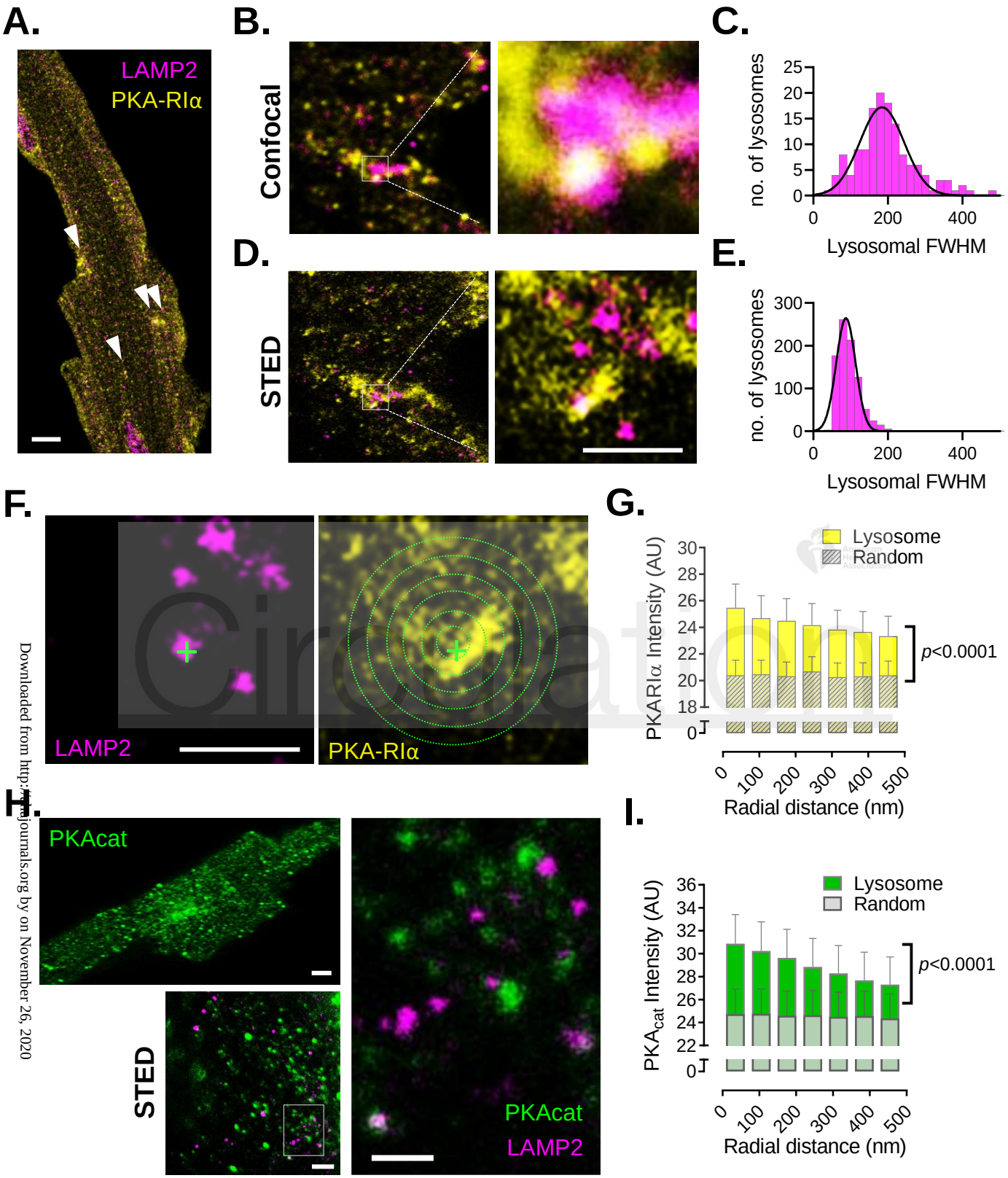

Figure 5

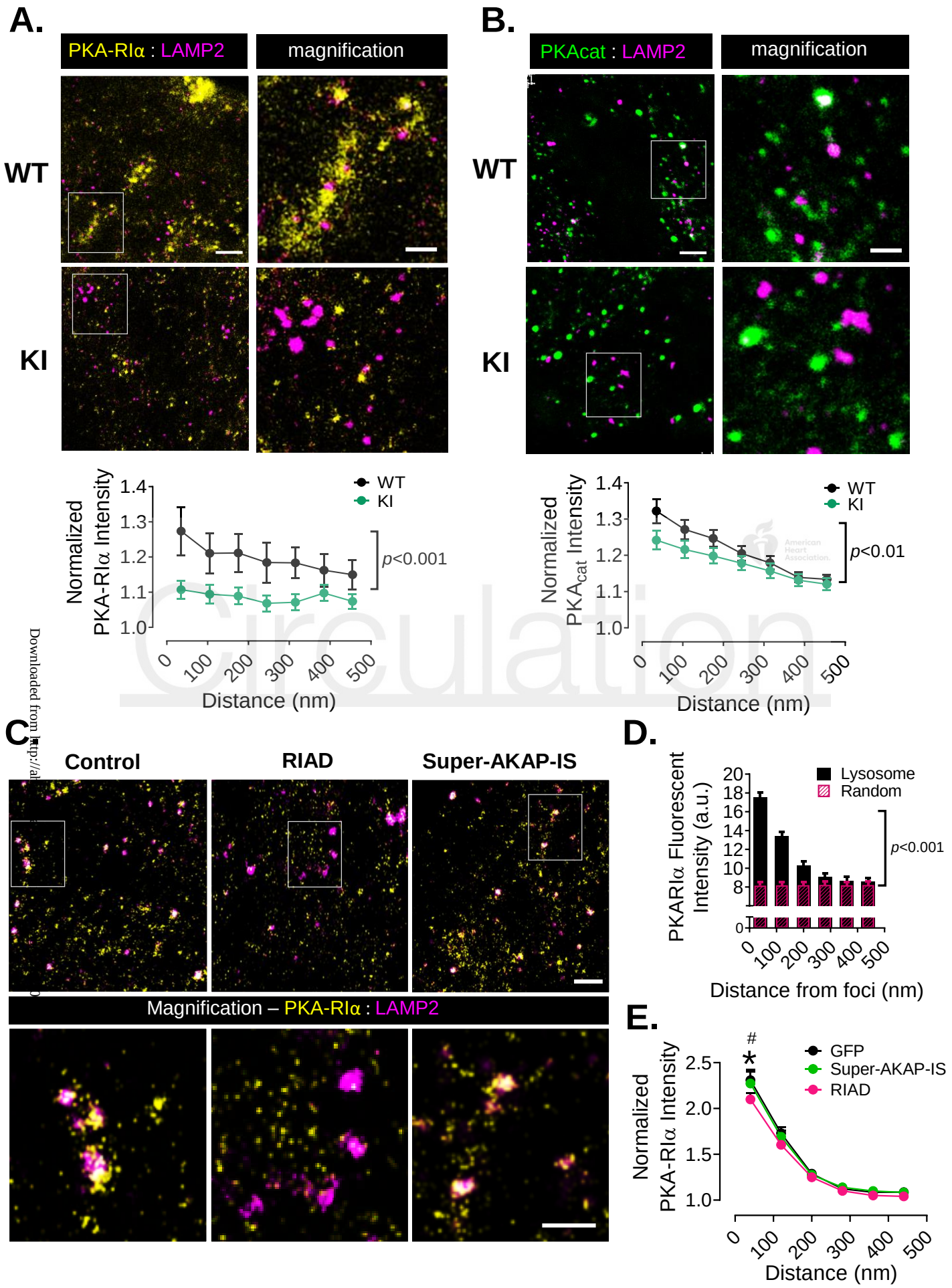

Figure 6

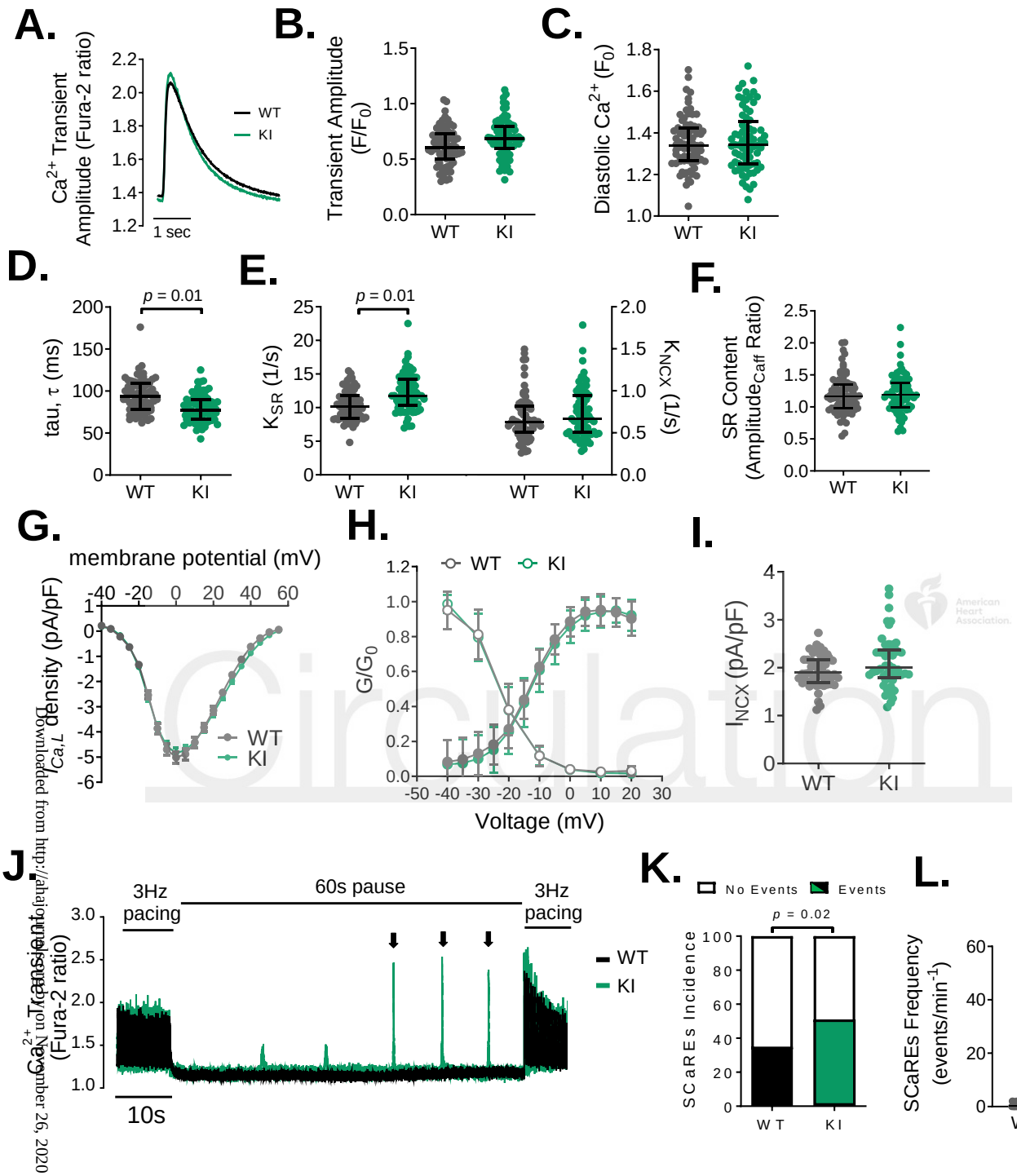

Figure 7

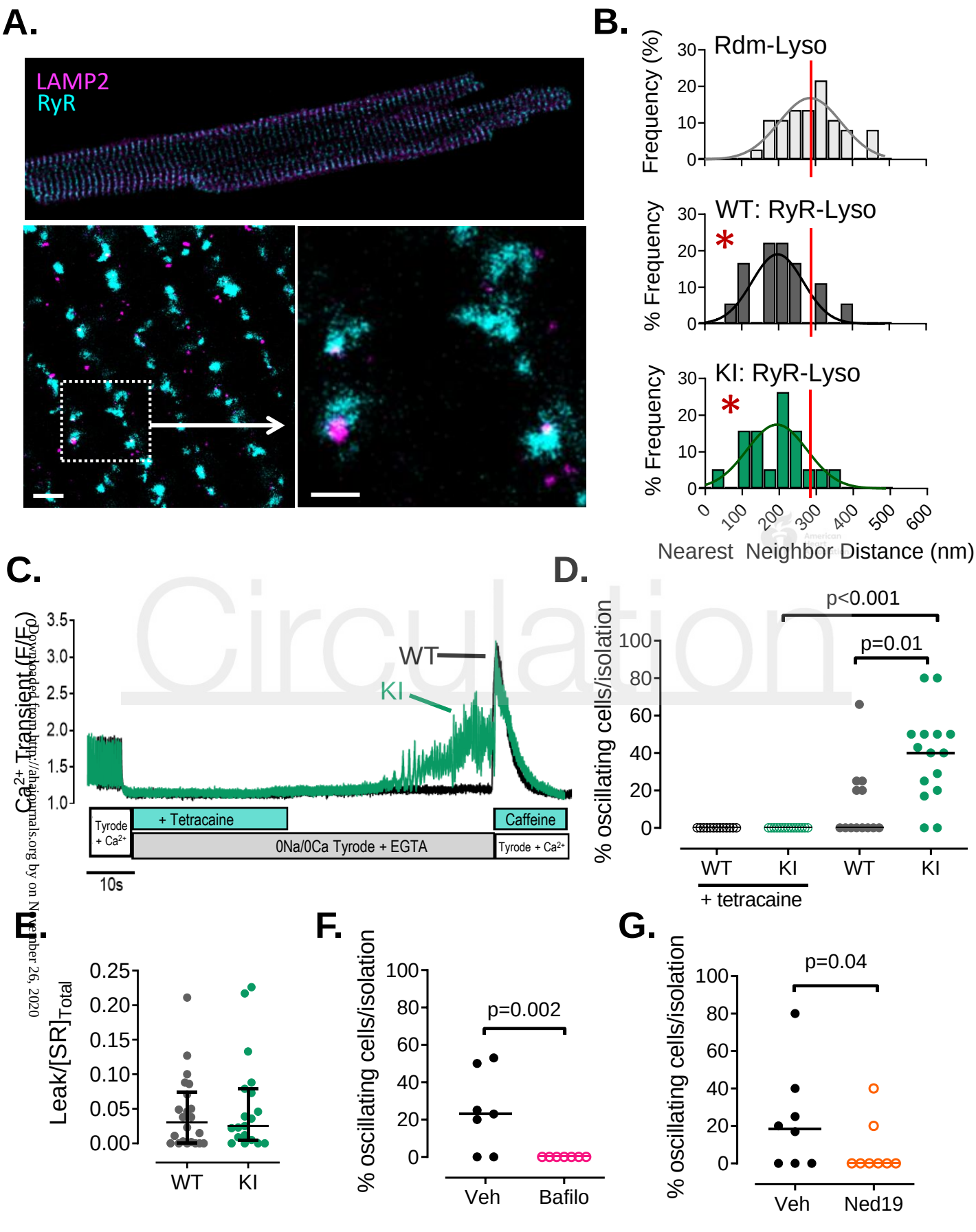

Figure 8